Energy performance of an open-joint ventilated façade compared with a conventional sealed cavity façade

Cristina Sanjuan [a], *María José Suárez* [b], *Marcos González* [b], *Jorge Pistono* [b], *Eduardo Blanco* [b*]

[a] *Department of Energy, Energy Efficiency in Buildings Unit, CIEMAT, 28040 Madrid, Spain*
[b] *Universidad de Oviedo, EDZE (Energía), Campus de Viesques, 33271 Gijón (Asturias) Spain*

[*]Corresponding author. Tel.: +34 985182103.
E-mail address: eblanco@uniovi.es (E. Blanco).

Abstract

The term "open-joint ventilated façades" refers to a building system in which coating material (metallic, ceramic, stone or composite) is hanged by means of a metallic-frame structure to the exterior face of the wall, creating an air cavity between wall and slabs. The coating material is placed in an arrangement of slabs and a series of thin joints from slab to slab to allow the surrounding air to enter and leave the cavity all along the wall. In addition to aesthetic and constructive reasons, the main interest in open joint ventilated façades is their ability to reduce cooling thermal loads. This is achieved by the buoyancy effect induced by solar radiation inside the ventilated cavity, where the air can enter or leave freely through the joints. This paper focuses on the phenomena produced on a typical open joint ventilated façade, and the comparison of its energy performance with that of a conventional sealed air cavity façade. The thermo fluid-dynamic behaviour of both systems has been analyzed with CFD techniques and the results of the 3D simulations conclude that open-joint ventilated façades can help to achieve important energy savings in climates with hot summers and mild winters.

Keywords: Ventilated façade, CFD, Energy-efficient building, Solar passive design.

1. Introduction

The Open-Joint Ventilated Façade (OJVF) is usually classified among the "Light Weight" or "Advanced Integrated Façades" (Fig. 1). They are replacing the conventional façade in many new buildings and particularly in the refurbishment of old ones. There are some reasons why these advanced façades have become so popular among architects, but perhaps the main one is because they can adopt nearly any colour and shape. Additionally to the aesthetic reasons, the set up of the exterior coating is very easy and fast, making them a very competitive system, especially in building restoration. With respect to their performance, the manufacturers argue that there are two main advantages. First, the ventilation reduces the problems posed by moisture, and secondly, under the effect of the solar radiation, the energy performance of these façade systems (mainly the OJVF) improves in relation to conventional façades. The Open-Joint Ventilated Façade has been pointed as a building system that can help to reach the objectives of the energy efficiency standards, especially in countries where the peak in power demand occurs during the summer period.

A conventional façade is usually composed of an exterior coating (brick veneer, stone or tiles fixed over a half brick wall, etc.), a closed air cavity about 5 to 10 cm, an insulation layer fixed over perforated brick or concrete blocks, and an interior finish (gypsum layer…). The exterior coating is frontally anchored to the floor slab in such a way that, theoretically at least, the thermal bridge is broken. The air chamber height is thus about the floor height. The closed air cavity is sometimes omitted or filled with insulation. In these cases, the thermal behaviour of the façade can be easily determined with a combined conduction coefficient. However, the conventional façade selected for this study includes the air cavity which is going to be a prime factor in the fluid dynamic analysis.

In the light weight façades, the exterior "light" coating material (metallic, ceramic, stone or composite) is "hanged" over the interior wall (insulation, perforated brick, finish; basically the same as before) by means of a metallic-frame structure or metallic bindings, leaving an air gap between them of similar dimensions to the one in the conventional façade. The air chamber height can be the whole building height, although it is usually broken by windows and other building elements, and sometimes even by the metallic-frame structure. In fact, in some advanced façades, the ventilation is quite restricted.

The main difference between the OJVF and other advanced façades is that, as a rule, the ventilated air chamber is only open to the exterior at the top and at the bottom while, in the OJVF, the exterior coating is placed in an arrangement of tiles or slabs and a series of thin gaps (joints) are shaped from slab to slab, enabling the exterior air to enter and leave the cavity all along the wall. A typical cross section of a conventional sealed cavity façade and an OJVF is shown in Fig. 2.

The improved thermal performance of the OJVF under radiation conditions relies on buoyancy: The slabs of the exterior coating are heated up and produce an ascending mass flow of air (by natural convection) that enters and leaves the cavity through the joints. This flow removes part of the heat loads, reducing the heat transfer to the indoor environment. This phenomenon takes also place if the openings are only at the bottom and top of the façade, but the efficiency is not as high due to the reduced flow and the higher temperatures attained at the upper section of the air gap. In the conventional sealed cavity façade, the heating of the

exterior layer produces a convective loop, with the flow raising along the hot wall and sinking along the cold wall. This effect is counterproductive, adding convection to the conduction and radiation heat transfer to the building interior.

However, there is very little information on the estimation of the heat transfer in OJVF under radiation. The manufacturers tend to forget this aspect or to provide "sealed" responses. Additionally, when there is no solar radiation, an OJVF could offer a lower insulation than a sealed cavity façade, mainly in winter; but that is another aspect not found in the brochures. Moreover, the building standards consider this façades, by default, as ordinary ventilated or slightly ventilated air chamber façades without taking into account the fluid behaviour. But, as the OJVF are more expensive than the conventional façades, their respective thermal efficiencies should not be neglected.

The main objective of this work is to investigate the thermal and fluid dynamic phenomena taking place in OJVF under solar radiation, and to appoint a methodology to quantify the energy savings produced by an OJVF in contrast to a conventional façade. The determination of the linked thermal and fluid dynamic behaviour of the flow in the open joint air gap is quite a challenge, compared to the sealed cavity or even the top and bottom ventilated façades. The inlet and outlet flow through the joints all along the façade faces the analytical methods, making compulsory the use of CFD tools to obtain a detailed model.

Due to the extent of the subject, the study has been developed over a particular set of comparable geometries, and with specific climatic conditions; however, special care has been taken to avoid assumptions limiting its application. The choice of the conventional facade to perform the comparison is based in the fact that the physical characteristics of both facades are similar and their costs are not too far apart, so building designers use them indistinctly.

2. Literature review

There are several studies (usually provided by the façade manufacturers) about the physical properties of the materials employed in the OJVF: conductivity, elasticity, fire resistance… and relative to the mechanical characteristics of the assembly but, to the authors knowledge, excluding their previous partial works (Gonzalez et al. 2008a and 2008b), no reference to the thermal behaviour nor the specific fluid dynamic phenomena existing in the Open Joint Ventilated Façades has been found. There are a great deal of papers in the category of "ventilated façade", related to Double Skin Ventilated Façades, Building Integrated Photovoltaic, Trombe and Solar Walls, Façade Solar collectors, and a few of them to Light Weight (bottom and top) ventilated façades. Most of them differ substantially from the OJVF in their geometry, architectural application and energy purpose, and all of them in the fluid dynamic features. Nevertheless, there are certain similarities that have been very useful for this study. For these reasons, this paper makes full use of the ideas collected in those parallel systems.

Before entering in the specific literature, it is worth to mention some basic investigations, applying the fundamental studies on heat transfer inside cavities, to façade elements. For instance, Lorente (2002) expand upon the analytical models to determine heat losses through building walls with closed, open and deformable cavities. Manz (2003) investigated numerically the pure natural convection heat transfer of tall rectangular cavities with different aspect ratios and Rayleigh numbers. Xaman et al. (2005) employed a computational approach to the laminar and turbulent natural convection flow in a two-dimensional tall rectangular cavity heated on a vertical side. Also, Gan (2006) developed a CFD simulation of buoyancy-induced flow in open cavities.

Beginning now with the most cited topic, the Double Skin Ventilated Façades (DSVF) can be considered as a singular solution, aesthetically different from conventional facades. They are usually composed of a double glazed wall (also described as Double Glazed Ventilated Façades DGVF) with a wide separation, and frequently with shadow elements in-between. They use to have adjustable openings, located in the upper and lower sides of the façade, both to the exterior and interior, employed to regulate the building ventilation and for energy collection purposes. Actually, an appreciable amount of the research on DSVF is directed to determine the best control strategies.

Some models, which have been developed to analyse the performance of DSVF, apply analytical methods to obtain approximate solutions: Balocco (2002) and Ciampi et al. (2003). Later, Balocco (2004) has also approached the problem using dimensional analysis. Design parameters and correlations presented by Pappas and Zhai (2008) are of a particular interest. More detailed models have been reported by authors that have analyzed double glazed ventilated facades with computational fluid dynamic techniques. Manz (2004), included convection, conduction and radiation to his already mentioned research, to model double facades made of glass layers with ventilated mid pane shading device; simulation results were compared with experimental data from an outdoor test facility. Safer et al. (2005) studied in a three-dimensional model, the fluid behaviour of a compact double-skin facade equipped with a venetian blind and forced ventilation. Recently authors like Baldinelli (2009), Fuliotto et al. (2010) and Coussirat et al. (2008), have approached the problem of double glazed ventilated façades by means of CFD techniques and have validated the numerical results using experimental data from real façades. Notwithstanding the differences with the OJVF, some useful information about the radiation and turbulence models and about the setting of the boundary conditions has been extracted from the previous articles.

The Building-Integrated Photovoltaic System (BIPV), arise from the substitution of the exterior skin of the DSVF with photovoltaic modules, either opaque or semi-transparent. Usually there is a wide air gap with openings at the bottom and top. In this case, the goal is to improve the panels cooling to increase its efficiency. The cost of these systems has relegated them to emblematic buildings. However, this topic also holds an extensive literature. The articles of Krauter et al. (1999), and Li and Lam (2008), for instance, study their performance and also the economic aspects. Brinkworth et al. (2000) apply an analytical model,

and Mei et al. (2003) make use of the TRNSYS software. Also, many authors have developed numerical models, validated with experimental results: Moshfegh and Sandberg (1998), Charron and Athienitis (2006) and Liao et al. (2007), for example.

Trombe Walls, Solar Walls and Façade Solar collectors are described in bioclimatic architecture as passive solar air heating systems. A comprehensive review can be found in Chan et al. (2010), with references to installations and published performances. The mathematical models for predicting solar air heaters are analyzed by Tchinda (2009).

Trombe Walls are intended to collect solar heat. They are typically built with a massive inner wall and an exterior glass front. The openings, always at the bottom and top and sometimes only to the interior, can be adjusted. The function of the inner wall is to gather the energy and to deliver it to the building with an appropriate delay (at night). Numerous references can be found about analytical global energy balances (Zrikem and Bilgen 1987, Mootz and Bezian 1996), numerical studies with finite differences and finite volumes (Mootz and Bezian 1996, Fang and Li 2000, Zalewski et al. 2002, Shen et al. 2007) and detailed experiments (Zalewski et al. 2002, Burek and Habeb 2007).

The term Solar Wall was normally applied to Trombe Walls but, nowadays, it is commercially employed in reference to Façade Solar collectors. This solution makes use of a kind of Light Weight ventilated façade, with a perforated dark-coloured metallic exterior cladding. This collector is known as unglazed perforated-absorber collector or Unglazed Transpired solar Collector (UTC). The essence of its operation is as follows: the metal cladding is heated by solar radiation; with the help of ventilation fans, the air is drawn to the top of the façade through the holes of the transpired metal sheet, absorbing the solar heat; finally this air is directly distributed into the building or conducted to the HVAC as preheated fresh air. This technology has been installed on a large number of sites and recommended by the International Energy Agency (IEA) (Cali et al. 1999) and the National Renewable Energy Laboratory (NREL, 1998). About the research on this topic, the basic theory for unglazed transpired collector is explained in detail by Kutscher et al. (1993) and Hollands (1998), and Cao et al. (1993) and Golneshan and Hollands (1998) reported the fundamental heat exchange correlations based on experimental results. Recently, Augustus Leon and Kumar (2007), have done a good review and have also developed an analytical model to determine its thermal performance.

Geometrically, the Unglazed Transpired solar collectors may seem very similar to the OJVF but, actually, the differences and operation made them nearly opposite. In the UTC the external cladding is meant to absorb heat instead of insulate, the air gap is wider (15 to 30 cm), the holes are not the slabs joints but many tiny holes or slits, and, most important, the air is drawn through "all" the holes by a fan, making forced convection the main heat transfer mechanism. Furthermore, the wind effect is usually negative on the UTC, and it is an important research subject, while the worst conditions for an OJVF take place in calm weather (Fleck et al. 2002, Nore et al. 2010, Defraeye et al. 2011).

To finish with this quick review, on Light Weight (bottom and top) ventilated façades it is noteworthy the work of Griffith (2006), who proposed a model to analyse ventilated cavities with an opaque outer layer. A good agreement has been found with experimental results (Naboni 2007), and other calculation methodologies (Gonzalez et al. 2008b). This model has been adopted by the EnergyPlus simulation package (EnergyPlus, 2008). It is also significant the CFD modelling of a 2D ventilated ceramic façade carried out by Mesado et al. (2010).

The aforementioned studies help to understand the phenomena entailed in OJVF, however, the physical and operational differences (opening locations, cavity thickness, material properties, air source…) produce substantial differences in the thermal and fluid dynamic behaviour, giving rise to dissimilar phenomena, and requiring diverse models. For instance, in the case of bottom and top ventilated façades, the upward flow is continuous, homogeneous and symmetrical along the wall, while the OJVF are marked by localized discontinuities at the joints, which turn the flow much more complex, demanding, among other things, a finer mesh. Or, in contrast to the fan induced flow of the transpired collectors, the OJVF requires more elaborate boundary conditions and solution procedures, together with an expanded domain.

3. Overview of the OJVF heat transfer phenomena

In this section, a generic description of the heat transfer problem in the OJVF is developed. The radiation, convective and conductive heat flows are basically described and the global energy balances for the wall components are presented in order to clarify the different processes involved in the phenomenon. In the model generated for this study - developed in the next section- the heat fluxes have been calculated using a CFD code. Each heat flow [W] has been calculated integrating the punctual heat fluxes [W/m^2] over the façade front, as it changes, among other things, with the punctual solid temperature and the air velocity next to the surface.

The heat transfer trough a façade with an air gap, exposed to solar radiation is represented in Fig. 3 (conduction through the solid walls has not been pictured to simplify the figure). The phenomena are basically the same in a conventional sealed cavity façade and in an OJVF; the main difference resides in the air conditions and behaviour inside the cavity. To study this problem, the two solid blocks (external layer and inner wall) and the air gap are analyzed separately.

The external layer receives the solar radiation; part of this radiation is immediately reflected in a specular or diffuse form -depending on the surface characteristics-, and part is absorbed. At the outside there is another radiation flow, due to the temperature difference between the surface and the environment. This radiation is mainly diffuse and it is sometimes considered together with the solar radiation reflected in diffuse form. Its value is influenced by the sky and the objects at the front of the façade. As an approximation it could be calculated as the radiation between two parallel surfaces, one at the external layer temperature and the other at the exterior air temperature. There is also convective heat transfer between the layer and the exterior

air, roughly proportional to the temperature differences, although a natural convention on a vertical surface would be a better approximation.

At the interior side there is radiation heat transfer between the external layer and the inner wall, and also there is convection between the inward surface of the layer and the air gap. When the global inlet heat flow at the layer is positive, its temperature increases (intensifying the outlet flows) and when the global inlet flow is negative, the layer temperature decreases (reducing the outlet flows). When the steady state is achieved, the inlet heat flow at one side should be equal to the outlet heat flow at the other side. Assuming inlet flows as positive, the steady state equation of the exterior slab can be expressed as:

$$Q_{Solar} + Q_{Refl} + Q_{Rad\ eL\text{-}env} + Q_{Conv\ eL\text{-}env} + Q_{Rad\ eL\text{-}iW} + Q_{Conv\ eL\text{-}gap} = 0 \qquad (1)$$

Where Q is heat flow [W], and the sub-indexes:
Solar: solar radiation
Refl: directly reflected solar radiation
Rad eL-env: Radiation between the external layer (*eL*) and the environment
Conv eL-env: Convection between the external layer and the environment (air at the façade exterior)
Rad eL-iW: Radiation between the external layer and the inner mass wall (*iW*)
Conv eL-gap: Convection between the external layer and the air inside the cavity (*gap*)

Joining together the terms of each surface, excluding the solar radiation:

$$Q_{Solar} + Q_{eL\text{-}ext} + Q_{eL\text{-}int} = 0 \qquad (2)$$

The term *eL-ext* (external Layer – exterior) combines the reflexion, the radiation with the environment and the convection with the air at the façade exterior, and the term *eL-int* (external Layer – interior) combines the radiation between the external layer and the inner wall, and the convection with the air cavity.

The phenomena at the inner wall of the façade are quite similar, except for the solar radiation and reflexion. At the gap side there is radiation heat exchange with the external layer and convective heat flow with the air at the cavity. At the room side there is radiation with the objects and other walls of the room, and convection with the air in the room. The steady state equation of this wall is:

$$Q_{Rad\ iW\text{-}eL} + Q_{Conv\ iW\text{-}gap} + Q_{Rad\ iW\text{-}room} + Q_{Conv\ iW\text{-}room} = 0 \qquad (3)$$

Rad iW-eL: Radiation between the inner wall and the external layer
Conv iW-gap: Convection between the inner wall and the air inside the cavity
Rad iW-room: Radiation between the inner wall and the room
Conv iW-room: Convection between the inner mass wall and the room

If the terms of each surface are joined together, each term is equal to the net heat flow to the room (with opposite signs):

$$Q_{iW\text{-}int} = - Q_{iW\text{-}room} = Q_{Room} \qquad (4)$$

In the above equation, the term *iW-int* (inner Wall – interior) combines the radiation between the inner wall and the external layer, with the convection to the air cavity, and the term *iW-room* (inner Wall – room) combines the radiation between the inner wall and the room, with the convection to the air in the room. The last term represents the total heat flow to the room.

As it can be seen in Fig. 4, the radical difference between the sealed cavity façade and the open joint façade resides in the air behaviour at the gap. In the conventional façade, a convective loop is developed, where the air near the external layer gets heated and ascends, while the air near the inner wall is cooled and descends (if the external layer is cooler than the inner wall, the loop is counterclockwise). As the cavity is sealed, the convective heat transfer between the external layer and the air in the gap has the same value and opposite sign as the convective heat transfer between the inner wall and the air.

$$- Q_{Conv\ eL\text{-}gap} = Q_{Conv\ iW\text{-}gap} \qquad (5)$$

As the same can be said about the radiant flows between the surfaces, all the heat released by the interior surface of the external layer (negative with the assumed convention) is absorbed by the inner wall (positive) and transmitted to the room (or vice versa if the heat goes from the room to the exterior). Also, it can be inferred that the mean air temperature at the gap will be between the temperatures of the surfaces at both sides.

The behaviour at the OJVF is quite different. Air can come in and leave, and -assuming the external layer is hotter than the exterior air- part of the convective heat at the interior side of the slabs will be extracted to the atmosphere. Therefore, the value of the convective flow between the gap and the inner wall will be smaller:

$$- Q_{Conv\ eL\text{-}gap} = Q_{Conv\ iW\text{-}gap} + Q_{Vent} \qquad (6)$$

The term *Vent* represents the heat flow evacuated by ventilation out of the façade.

The mean air temperature at the cavity will be somewhere between the exterior temperature and the temperature of the inner surfaces at both sides of the gap, and it is therefore expected to have a lower value than in the conventional sealed cavity façade.

Strictly speaking, the heat fluxes -and the temperatures- change with height. In the sealed cavity the air at the gap heats while ascending next to the external layer and cools while descending next to the inner wall. In the open joint façade the air begins at the exterior temperature and heats while ascending. Also, the structure of the convective heat transfer at both sides of the slabs is different: in the sealed façade there is a relatively simple natural convection on a vertical surface while, at the OJVF, this convection is entangled with the inlet and outlet flow through the joints, with the air motion and thermal field strongly coupled and dependent on different geometric characteristics. All this makes that two dimensional or even tree dimensional differential equations should be used for a detailed study of this phenomenon.

The two extreme situations where the differences between the sealed façade and the OJVF can be better observed are summer weather ($T_{room} < T_{ext}$) with high solar radiation, and winter ($T_{room} > T_{ext}$) with little or no irradiation. In the first case, the solar radiation effectively heats the external layer and there is also a relatively high radiation between this layer and the inner wall. The air temperature inside the gap is higher in the sealed cavity than in the OJVF, and the heat transferred to the room is also larger. In the second case the external layer temperature is similar to the ambient temperature, the cavity air temperature in the OJVF is lower than in the sealed cavity, and the heat losses of the room are higher. In a general way, it can be stated that the OJVF is better for summer conditions, mainly at the sunny side of the building while the conventional sealed cavity façade is better for winter conditions. In any case, a quite detailed study is needed to see whether the advantages overcame the drawbacks.

4. Numerical model

The numerical model employs a Computational Fluid Dynamic code (FLUENT 6.3) to analyse the thermal and fluid dynamic phenomena taking place in OJVF in contrast to those present in a conventional (sealed cavity) façade. Special emphasis has been put to the behaviour of the air flow inside the air gap under solar radiation, but the solid materials have also been included in the simulation. To compare both façades, two similar three-dimensional geometries have been generated and tested with the same climatic conditions.

In the CFD model development, the precise geometry is built inside a domain including the relevant air zones. This domain is split in small cells, and appropriate boundary conditions are applied to the contours. The CFD code solves the Navier-Stokes differential equations, discretizing them, and determining iteratively the variables and fluxes in each cell.

4.1. Geometry materials and mesh

The OJVF simulated geometry (Fig. 5) comprises eight tiles in two columns of four so that vertical and horizontal joints can be analyzed. Each slab is 1.2 m wide 0.6 m high and 0.01 m thick (one of the dimensions commercially used, although the thickness changes with materials and manufacturers). They are separated by joints of 5 mm. The exterior coating layer is separated 0.05 m from the massive wall by the ventilated air cavity. The massive wall is composed of gypsum, a brick layer and exterior insulation with a total thickness of 0.15 m and a combined conductivity of 0.046 W/mK. Table 1 gives the thickness and thermal properties of all the layers. The fluid (air) has the standard properties at atmospheric pressure (101325 Pa absolute), its density obviously varies with temperature but, the pressure variations are so small, that the effect is negligible. The height of the simulated domain is one of the most influencing parameters on the thermal behaviour of the façade. As a starting point, a height of 2.425 m has been selected because it is a representative distance between floors. Unlike most existing models for ventilated facades, the computational domain includes a big air volume attached to the exterior layer of the façade. This zone allows the correct simulation of the outdoor air natural convection and the flow inlet through the joints. Vertical symmetry has been applied in the model, so that the simulated volume is half the real geometry.

To study the heat transfer problem in the case of a conventional wall, a 3D model with the same dimensions has been created to simulate the convective loop inside the sealed air cavity. The only difference with respect to the OJVF model relies in the exterior coating which is continuous (without joints between slabs).

A structured hexahedral grid about 950000 cells was generated over both geometries, with a refined grid in the area of the joints and the air cavity, where more complex fluid structures are expected. A view of the mesh over the slabs in the OJVF can be seen in Fig. 6. In addition, the denser mesh near the joints can be discerned.

4.2. Mathematical models

The CFD software solves the Navier–Stokes equations (including the energy conservation equation) using a finite volume method. The details of the equations discretization and solution procedures can be found in the software documentation (Fluent 2006).

Turbulence effects are included using a Reynolds average (RANS) approach, with the *K-ε* (RNG) turbulence model (Launder and Spalding, 1974; Choudhury, 1993). This method has been recommended in the literature as a good compromise between accuracy and solving time (Chen, 1995), and it has been extensively validated for channel flows (ventilated facades) in recent works from Xaman et al. (2005), Coussirat et al. (2008), Fuliotto et al. (2010) and Patania et al. (2010).

The discrete ordinates model (Chui and Raithby, 1993) has been chosen for the radiation. This model transforms the radiation transfer equation into a transport equation for radiation intensity in the spatial coordinates, solving as many transport equations as there are direction vectors associated with a number of discrete solid angles.

Gravitational body forces were activated within the momentum equation (Coussirat et al. 2008), using the Boussinesq approximation (Gray and Giorgini, 1976) to model buoyancy effects. This approximation assists the convergence of the solution when free convection is the main force driving the fluid, and helps to reduce computation time.

To minimize numerical errors, the set of equations were solved using a pressure-based double-precision solver and second order upwind discretization schemes were imposed on all the transport equations.

4.3. Boundary conditions

Fig. 5 shows a sketch of the boundary conditions imposed in the model. The incident radiation has been included as an internal heat source in the exterior face of the slabs; this value is thus the absorbed radiation: the component perpendicular to the façade of the solar minus the reflected radiation. The thermal boundary condition from the interior layer of the mass wall to the room was imposed with an indoor temperature and a combined convection-radiation heat transfer coefficient of 8 W/m^2K (an average from the building standards of several countries). The exterior front and bottom air boundaries have been defined as constant temperature, no flow surfaces. The domain top has constant (atmospheric) pressure and, for the inlet flow, the same exterior temperature as the rest of the air boundaries (the outlet flow temperature is a result of the calculation). Symmetry was imposed in both laterals. The room combined coefficient is the only one used in the simulation; the heat transfer due to convection and radiation in the rest of the surfaces is directly calculated during the simulation using the materials properties and the solution variables (temperature, velocity…) in each cell.

Two series of tests have been carried out for both OJVF and sealed cavity façade. The first ones are steady state simulations directed to understand the phenomena involved, and the others are quasi-steady state simulations to compare the energy performance of both systems.

For the first group, two temperature conditions were selected, representing summer (T_{room} = 24ºC, T_{ext} = 30ºC) and winter (T_{room} = 24ºC, T_{ext} = 8ºC) weather. The room temperature is a little high for winter conditions, but it has been maintained to better compare the effects of the outer part of the façade. The (absorbed) solar radiation ranges from 0 to 800 W/m^2. The radiation values above 400 W/m^2 are high for summer, but not for winter, because the sun inclination is lower (more perpendicular to the façade).

The second group comprises two sets of simulations with the exterior temperature and the solar radiation varying hourly: one for a typical day of summer and another for a typical day of winter. The data corresponds to Madrid (Spain) (Zarzalejo et al. 1995), which is a good example of Continental Mediterranean Climate (Köppen climate classification: Csa. Kottek et al. 2006) with cold winters, hot summers, low precipitation and high levels of solar radiation. The interior temperature of the building has been kept to a constant value of 24ºC.

5. Results

The two following sections analyse the fluid dynamic and thermal phenomena emerging in the OJVF on the basis of the data obtained from the first series of tests, mainly with and absorbed radiation of 400 W/m^2, which is representative of the higher values of the day during summer.

5.1. Fluid dynamic behaviour of OJVF

In the OJVF, as the incident radiation increases the temperature of the slabs and, consequently, of the air in the gap, the buoyancy forces generate an ascending flow in the cavity. Fig. 7 shows the horizontally averaged total velocity magnitude and z velocity component of the air flow at the middle vertical plane, along the cavity in the OJVF for summer conditions. The relation between them indicates that the velocity vertical component is the main one in the ventilated cavity flow. The air enters the cavity mainly through the joints of the lower slabs, and leaves the cavity through the joints of the upper slabs. The maximum flow rate is reached about the central part of the façade, although there is no horizontal symmetry. The position of the horizontal joints is clearly defined because they produce very high gradients in the velocity magnitude. The slope of the curves at the middle of the slabs indicates that there is also a significant inflow through the vertical joints.

Fig. 8 compares the z-velocity profiles in the cavity of the OJVF and the conventional façade. The air flow in the OJVF is ascending in the whole width and does not form a convective loop as in the sealed cavity façade. Moreover, the profiles show much higher velocity values in the case of OJVF. These two characteristics favour the heat removal from the cavity walls, which is one of the most claimed advantages of OJVF under radiation conditions.

The ventilation mass flow rate in the cavity, as a function of the solar (absorbed) radiation, is presented in Fig. 9. It has been calculated at the central height of the OJVF for a frontal section of one slab. As it would be expected, the chimney effect increases with the solar radiation, but not linearly because as the radiation (and the slabs temperature) increases, so does the heat flow from the external layer to the exterior (cf. Eq. 2). Also, for each radiation value, the mass flow rate in winter is smaller than in summer because the same heat flow is larger due to the cooler exterior temperature.

5.2. Thermal behaviour of the OJVF

The contrast in the vertical temperature distribution inside the air cavity of the ventilated and the sealed façade can be seen in Fig. 10. The curves correspond to different width positions: next to the slabs, middle and next to the inner wall. In the OJVF the outdoor air entering the cavity through the joints at the lower part is cooler not only than the external layer, which has been heated by direct sun radiation, but also cooler than the inner wall, heated by radiation from the external layer. It produces a ventilation effect, removing heat from both walls. If the air temperature were higher than the interior temperature (which happens with lower radiations or with higher outdoor temperatures), the air flow in the OJVF will cool the external layer and heat the inner wall. Still the air temperature in the cavity remains lower than in the conventional wall, and the heat transferred to the room is therefore lower. In the sealed cavity of a conventional façade the convective loop produces a heat transfer from the hottest surface (usually the external layer heated by radiation) to the cooler surface. The air inside the sealed cavity remains at a temperature between both, which is higher than in the case of OJVF. The temperatures in this figure may seem too high but it has to be taken into account that they correspond to an air gap with exterior temperature of 30ºC and a high radiation (400 W/m^2 of absorbed radiation are obtained with a summer total radiation about 800 W/m^2).

Fig. 11 represents the heat flux transmitted to the interior of the room for the same conditions. Fluxes entering the building have been set as positive. The heat flux in the conventional façade is relatively uniform along the height of the facade, while in the OJVF, it increases as the air inside the cavity raises its temperature. The total heat flow (integrating in height and multiplying by the frontal length) is significantly larger in the case of the sealed cavity façade.

In Fig. 12, the heat fluxes on the external layer (slabs) to the exterior and to the air cavity have been represented for both OJVF and the sealed façade (once integrated, they correspond to second and third term of Eq. 2). The radiation flux absorbed in the slabs is dissipated to the exterior but also to the cavity. In the case of sealed façade, although the heat flux to the exterior is larger than in the OJVF, all the remaining heat is transmitted to the inner wall (through radiation and convection: Eq. 5) and therefore to the room. In contrast, in the OJVF, the heat transmitted from the slabs to cavity is larger but it is mainly gathered by the ascending ventilation flow inside the cavity and conveyed to the exterior (Eq. 6).

5.3. Energy performance of the OJVF

The simulations presented in this section have been carried out under quasi-steady conditions, using the data (outside temperature and solar radiation) of a typical winter day and a typical summer day in Madrid, and for a south and a north oriented facades (on the northern hemisphere: sunny and shadow side)

Fig. 13 compares the energy performance of both façade systems along the selected typical days. The heat fluxes to the room for both, OJVF and conventional sealed façade are hourly plotted for the two orientations. This heat flux has been calculated as the integrated heat flow, divided by the façade frontal surface. The solar incident radiation on the south façade and the outdoor temperature are also included in the graph. Heat gains have been plotted as positive values and heat losses as negative.

It has to be noted that the temperature and solar radiation used in the simulations are not extreme conditions because the data have been taken from the “typical meteorological year”, which is a 10 years average developed to analyze buildings energy efficiency. The temperature ranges from 21.1ºC to 29.5ºC in summer, and from 7.2ºC to 14.4ºC in winter, while the maximum solar radiation perpendicular to the wall is 432 W/m^2 and 834 W/m^2 respectively (higher in winter because the sun is nearer to the horizon). For the selected days, there are 14 hours with daylight in summer and 10 hours with daylight in winter.

In summer there is relatively little heat flux (positive or negative) through the north façade during the whole day, and the same can be said about the south facade at night. This happens, because in those conditions the main parameter is the outdoor temperature, which does not deviate much from the room temperature. On the other hand, during the day, the influence of the solar radiation is clearly noticed, and the advantages of the OJVF are evident in the south facade.

During the typical winter day, there is a substantial heat loss through the north and south facades at night time, because the exterior temperature is rather lower than the room temperature. Here the OJVF is a clear disadvantage. Only at the south façade, during the daylight hours (when the heat flux is positive), the OJVF shows its properties.

In table 2, the heat transferred to the room has been integrated for the typical days studied, quantifying the trends commented above. The values are per square meter of façade. The table includes data corresponding to the heat transferred to the room during the day and during the night, as well as the energy required, for both facade systems at the two orientations. The energy required

has been calculated for the whole day adding the heat losses (absolute value) to the heat gains divided by three. This calculation is based on the assumption that the energy needed for cooling is roughly one third of the required for heating (this means an average C.O.P. of 3); assuming the same kind of energy (electricity for example) is used in both cases.

The best performance of the OJVF at south facade happens in the summer period. During the radiation hours, 26% less heat is transferred into the room in comparison with the conventional sealed facade. Additionally, the losses at night can be considered as negligible. With respect to the north facade, the OJVF behaves slightly better during day time and has only small differences at night.

In winter, 58% less heat is gained through the south façade with the OJVF, but the heat losses at the north side are proportionally higher. Also, during the winter nights, the heat losses are 50% higher through the OJVF for both orientations.

The energy required for heating and cooling during the whole day in summer is 20% lower for the OJVF at south side and almost the same at north side. In winter, on the other hand, the OJVF needs 27% more energy at both sides. The sum of the energy required in the typical day of summer and winter, shows that the OJVF demands 11% more energy at the south side and 51% more at the north side.

It has to be taken into account that this analysis has been done over a specific OJVF geometry, and for the climatic conditions of Madrid. Nevertheless, in a general way, it could be said that the OJVF could be a better system than the sealed façade, mainly in southern facades of buildings, in climates with hot summers and mild winters, but they behave poorly in harsh winters, especially at the north side. In fact, in Mediterranean Countries, it is usual to find buildings (as for example office buildings or public buildings with high occupancy) that require cooling in winter in addition to summer. In these buildings an OJVF at the southern facades could be an economically attractive alternative.

Summarizing, the OJVF displays better thermal characteristics than the conventional sealed cavity façade against the solar radiation (south orientations), because buoyancy forces generate a ventilation along the cavity that removes the heat from the wall. On the other hand, the sealed façade is a better insulation in the absence of solar radiation (north and night). However, if there are other factors commending it, as the aesthetic appearance, it should be possible to reduce the negative effects of the OJVF in northern orientations sealing the joints or improving the insulation thickness of the inner mass wall.

6. Conclusions

The three-dimensional CFD model developed to simulate a typical Open Joint Ventilated Façade has enabled a better understanding of the ventilation effect induced by the solar radiation in the air gap of the façade. Velocity profiles, together with temperature and heat flux distributions have been compared with those obtained in a conventional sealed cavity façade. The model has been also used to compare the thermal performance of both façades for the specific climatic conditions of Madrid (Spain).

The results conclude that temperatures in OJVF under radiation conditions are lower than the temperatures in the conventional façades with sealed cavity, and consequently less heat is transferred to the building interior. In northern facades, the sealed cavity facade has a better behaviour than the OJVF, most of all with very high or very low exterior temperatures.

The comparison of the thermal performance of the specific OJVF and conventional façade analysed in this article shows that the open joint façade has heat gains 26% lower through the south facade during the daylight hours in the typical summer day selected. However, the same analyses also show that the OJVF can have as much as 50% more heat losses through the north facade at night in the typical winter day tested.

At this point, it is not possible to give a definite criterion, because it is still necessary to evaluate the overall year performance of the specific OJVF geometry for each climate conditions, taking into account building costs and the price of the energy used for heating and cooling. Nevertheless, the data found in this study show that the OJVF could be a more energy efficient system than the conventional sealed façade, and help to reduce the cooling needs, mainly for south orientations in places with hot summers and mild winters.

7. Acknowledgments.

This research was done under the PSE-ARFRISOL project. PSE-ARFRISOL (reference PSE-120000-2005-1) is a scientific-technical research project of singular character, supported by the National Research, Development and Innovation Plan (Plan Nacional de I+D+I) 2004-2007 from the Spanish Education and Science Authority (Ministerio de Eduación y Ciencia), funded with European Regional Development Funds (ERDF). The authors greatly thank all members of the ARFRISOL consortium for their support.

8. References

Augustus Leon, M., Kumar, S., 2007. Mathematical modeling and thermal performance analysis of unglazed transpired solar collectors. Solar Energy 81, 62-75.

Baldinelli, G., (2009). Double skin facades for warm climate regions: Analysis of a solution with an integrated movable shading system. Building and Environment 44, 1107-1118.

Balocco, C., 2002. A simple model to study ventilated façades energy performance. Energy and Buildings 34, 469-475.

Balocco, C., 2004. A non-dimensional analysis of a ventilated double façade energy performance. Energy and Buildings 36, 35-40.
Brinkworth, B.J., Marshall, R.H., Ibarahim, Z., 2000. A validated model of naturally ventilated PV cladding. Solar Energy 69 (1), 67-81.
Burek , S.A.M., Habeb, A., 2007. Air flow and thermal efficiency characteristics in solar chimneys and Trombe Walls. Energy and Buildings 39, 128-135.
Cali A, Kutscher CF, Dymond CS, Pfluger R, Hollick J, Kokko J, et al. 1999. A report of Task 14 Air Systems Working Group: low cost high performance solar air heating systems using perforated absorbers. Washington: International Energy Agency (IEA); Report No. SHC.T14.Air.1.
Cao, S., Hollands, K.G.T., Brundrett, E., 1993. Heat exchange effectiveness of unglazed transpired-plate solar collector in 2D flow. Proceedings of ISES Solar World Congress 1993, Budapest, Hungary, 5, 351-366.
Ciampi, M., Leccese, F., Tuoni, G., 2003. Ventilated façades energy performance in summer cooling of buildings. Solar Energy 75, 491-502.
Chan, H.Y., Riffat, S.B., Zhu, J., 2010. Review of passive solar heating and cooling technologies. Renewable and Sustainable Energy Reviews 14, 781-789.
Charron, R., Athienitis, A.K., 2006. A two-dimensional model of a double-façade with integrated photovoltaic panels. Transactions of the ASME, 128, 160-167.
Chen, Q., 1995. Comparison of different κ-ε models for indoor airflow computations. Numerical Heat Transfer, Part B 28, 353-369.
Choudhury, D., 1993. Introduction to the Renormalization Group Method and Turbulence Modeling. Fluent Inc. Technical Memorandum TM-107.
Chui, E.H., Raithby, G.D., 1993. Computation of radiant heat transfer on a non-orthogonal mesh using the finite-volume method. Numerical Heat Transfer, Part B 23, 269-288.
Coussirat, M., Guardo, A., Jou, E., Egusquiza, E., Cuerva, E., Alavedra, P., 2008. Performance and influence of numerical sub-models on the CFD simulation of free and forced convection in double-glazed ventilated facades. Energy and Buildings 40, 1781-1789.
Defraeye, T., Blocken, B., Carmeliet, J., 2011. Convective heat transfer coefficients for exterior building surfaces: Existing correlations and CFD modelling. Energy Conversion and Management 52, 512–522.
Energy Plus, 2008. Engineering Reference Manual, Building Technologies Program, U.S. Department of Energy (DOE).
Fang, X., Li, Y., 2000. Numerical simulation and sensitivity analysis of lattice passive solar heating walls. Solar Energy 69 (1), 55-66.
Fleck, B.A., Meier, R.M., Matovic, M.D., 2002. A field study of the wind effects on the performance of an unglazed transpired solar collector. Solar Energy 73 (3), 209-216.
Fluent, 2006. Fluent 6.3 Documentation. Lebanon, US: Fluent Inc..
Fuliotto, R., Cambuli, F., Mandas, N., Bacchin, N., Manara, G., Chen, Q., 2010. Experimental and numerical analysis of heat transfer and airflow on an interactive building façade. Energy and Buildings 42, 23-28.
Gan, G., 2006. Simulation of buoyancy-induced flow in open cavities for natural ventilation. Energy and Buildings 38, 410-420.
Golneshan, A.A., Hollands, K.G.T., 1998. Experiments on forced convection heat transfer from slotted transpired plates. Proceedings of CSME Forum 1998, Toronto, Canada, 1, 78-88.
González, M., Blanco, E., Río, J.L., Pistono, J., San Juan, C., 2008a. Numerical study on thermal and fluid dynamic behaviour of an open-joint ventilated façade. Proceedings of PLEA 2008 – 25th Conference on Passive and Low Energy Architecture, 22 - 24 October, Dublin, Ireland.
González, M., Blanco, E., Pistono, J., 2008b. Adjusting an energy simulation model by means of CFD techniques to analyze open-joint ventilated façades energy performance. Proceedings of WREC-X 2008 World Renewable Energy Congress, Glasgow, UK.
Gray, D.D., Giorgini, A., 1976. The validity of the Boussinesq approximation for liquids and gases. International Journal of Heat and Mass Transfer 19, 545-551.
Griffith, B., 2006. A model for naturally ventilated cavities on the exteriors of opaque building envelopes. Proceedings of SIMBUILD2006, Cambridge-Massachusetts, USA.
Hollands, K.G.T., 1998. Principles of the transpired-plate air heating collector: the SOLARWALL, renewable energy technologies in cold climates. Annual Meeting of the Solar Energy Society of Canada Inc. SESCI, Ottawa, 139-144.
Kottek, M., Grieser, J., Beck, C., Rudolf, B., Rubel, F., 2006. World Map of the Köppen–Geiger climate classification updated. Meteorologische Zeitschrift 15, 259–263.
Krauter, S., Guido Araújo, R., Schroer, S., Hanitsch, R., Salhi, M.J., Triebel, C., Lemoine, R., 1999. Combined photovoltaic and solar thermal systems for façade integration and building insulation. Solar Energy 67 (4-6), 239-248.
Kutscher, C.F., Christensen, C., Barker, G., 1993. Unglazed transpired solar collectors: heat loss theory. ASME Journal of Solar Engineering 115 (3), 182-188.
Launder, B.E., Spalding, D.B., 1974. The numerical computation of turbulent flows. Computer Methods in Applied Mechanics and Engineering 3, 269-289.

Li, D.H.W., Lam, T.N.T., 2008. An analysis of building energy performance and benefits using solar facades. Proceedings IMechE 222, Part A: J. Power and Energy, 299-308.
Liao, L., Athienitis, A.K., Candanedo, L., Park, K.W., Poissant, Y., Collins, M., 2007. Numerical and Experimental Study of Heat Transfer in a BIPV-Thermal System. Journal of Solar Energy Engineering 129, 423-430.
Lorente, S., 2002. Heat losses through building walls with closed, open and deformable cavities. International Journal of Energy Research 26, 611-632.
Manz, H., 2003. Numerical simulation of heat transfer by natural convection in cavities façade elements. Energy and Buildings 35, 305-311.
Manz, H. ,2004. Airflow patterns and thermal behaviour of mechanically ventilated glass double façades: Building and Environment 39 (9), 1023–1033.
Mei, L., Infield, D., Eicker, U., Fux, V., 2003. Thermal modelling of a building with an integrated ventilated PV façade. Energy and Buildings 35, 605-617.
Mesado, C., Chiva, S., Juliá, E., Hernandez, L., 2010. Two dimensional modelling with CFD of the behaviour of a ventilated ceramic facade. V European Conference on Computational Fluid Dynamics ECCOMAS CFD, 14-17 June 2010, Lisbon, Portugal.
Mootz, F., Bezian, J.J., 1996. Numerical Study of a ventilated façade panel. Solar Energy 57, (1), 29-36.
Moshfegh, B., Sandberg, M., 1998. Flow and heat transfer in the air gap between photovoltaic panels. Renewable and Sustainable Energy Reviews 2, 287-301.
Naboni, E., 2007. Ventilated opaque walls-A performance simulation method and assessment of simulated performance. Seminar Notes at Lawrence Berkeley National Laboratory Environmental Energy Technologies Division Berkeley, May 28, California, USA.
National Renewable Energy Laboratory, 1998. Transpired collectors (solar preheaters for outdoor ventilation air). Washington: The U.S Department of Energy.
Nore, K., Blocken, B., Thue, J.V., 2010. On CFD simulation of wind-induced airflow in narrow ventilated façade cavities: Coupled and decoupled simulations and modelling limitations. Building and Environment 45, 1834-1846.
Pappas, A., Zhai, Z., 2008. Numerical investigation on thermal performance and correlations of double skin façade with buoyancy-driven airflow. Energy and Buildings 40, 466-475.
Patania F., Gagliano A., Nocera F., Ferlito A., Galesi A., 2010. Thermofluid-dynamic analysis of ventilated facades, Energy and Buildings, 42 , 1148-1155
Safer, N., Woloszyn, M., Roux, J.J., 2005. Three-dimensional simulation with a CFD tool of the airflow phenomena in single floor double-skin facade equipped with a venetian blind. Solar Energy 79 (2), 193–203.
Shen, J., Lassue, S., Zalewski, L., Huang, D., 2007. Numerical study on thermal behavior of classical or composite Trombe solar walls. Energy and Buildings 39, 962-974.
Tchinda, R., 2009. A review of the mathematical models for predicting solar air heaters systems. Renewable and Sustainable Energy Reviews 13, 1734-1759.
Xamán J., Álvarez G., Lira L., Estrada C., 2005. Numerical study of heat transfer by laminar and turbulent natural convection in tall cavities of façade elements. Energy and Buildings 37 (7), 787-794.
Zalewski, L., Lassue, S., Duthoit, B., Butez, M., 2002. Study of solar walls – validating a simulation model. Building and Environment 37, 109-121.
Zarzalejo, L.F., Téllez, F.M., Palomo, E., Heras, M.R., 1995. Creation of typical meteorological years (TMY) for Southern Spanish cities. International Symposium Passive Cooling of Buildings. Athens, Greece.
Zrikem, Z., Bilgen, E., 1987. Theoretical study of a composite Trombe-Michel wall solar collector system. Solar Energy 39 (5), 409-419.

Figures and Tables

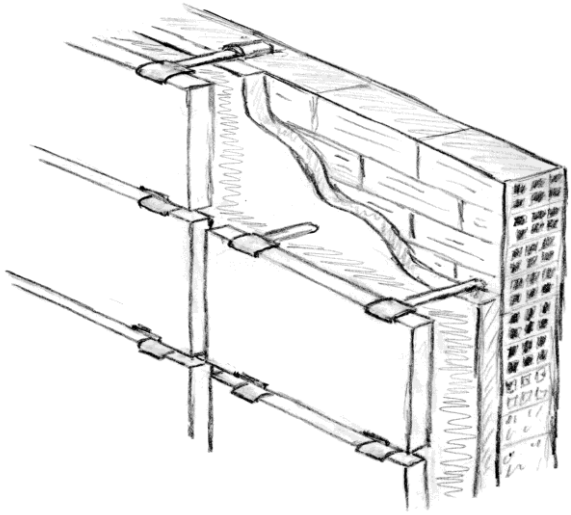

Fig. 1. Open-joint ventilated façade (the joints are exaggerated in the drawing)

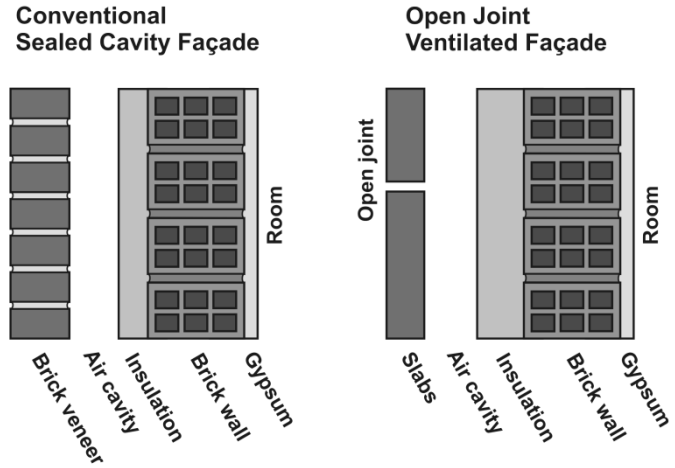

Fig. 2. Typical cross section of a sealed cavity and an open-joint ventilated façade (OJVF)

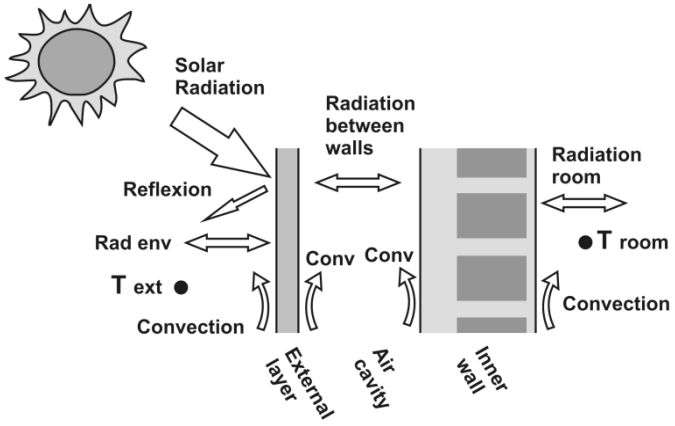

Fig. 3. Heat fluxes in a façade with an air cavity.

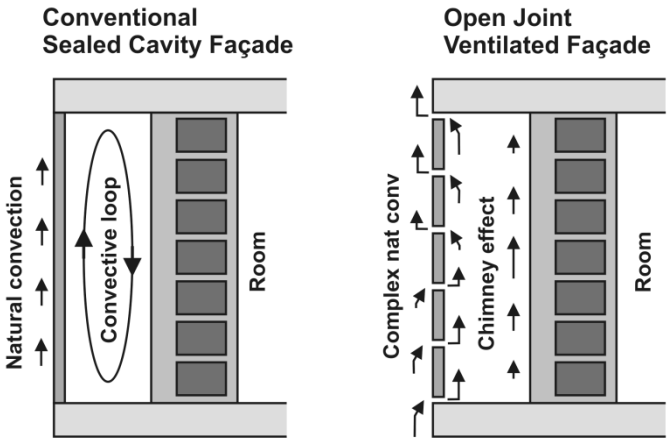

Fig. 4. Differences in heat transfer processes between a conventional sealed cavity façade and an OJVF.

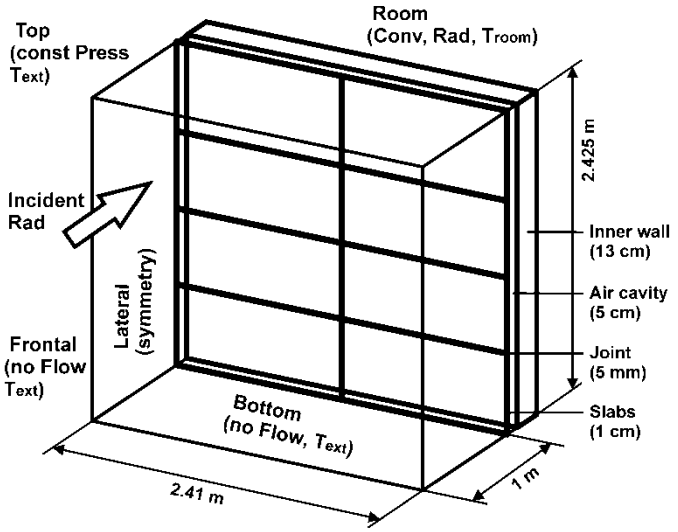

Fig 5. Model domain. Dimensions and boundary conditions.

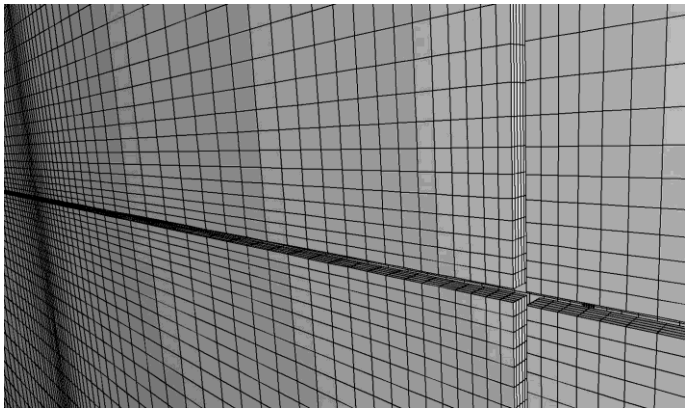

Fig. 6. Mesh over the slabs and horizontal and vertical joints.

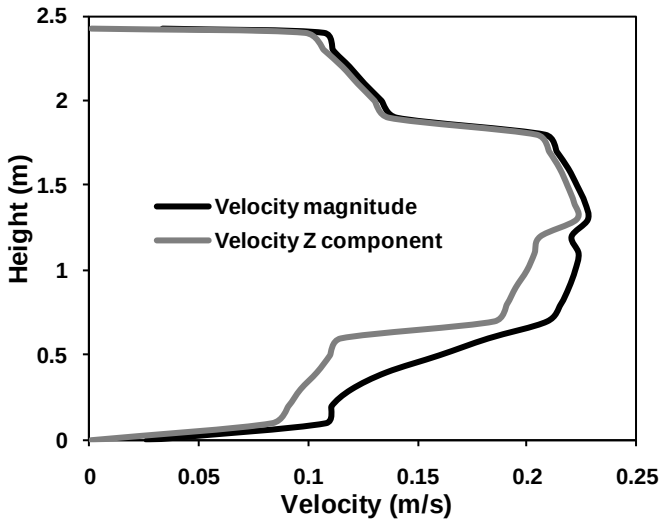

Fig. 7. Horizontally averaged velocity magnitude and Z velocity component, at the middle vertical plane in the OJVF. Summer conditions (24ºC room, 30ºC exterior, 400 W/m^2 absorbed solar radiation)

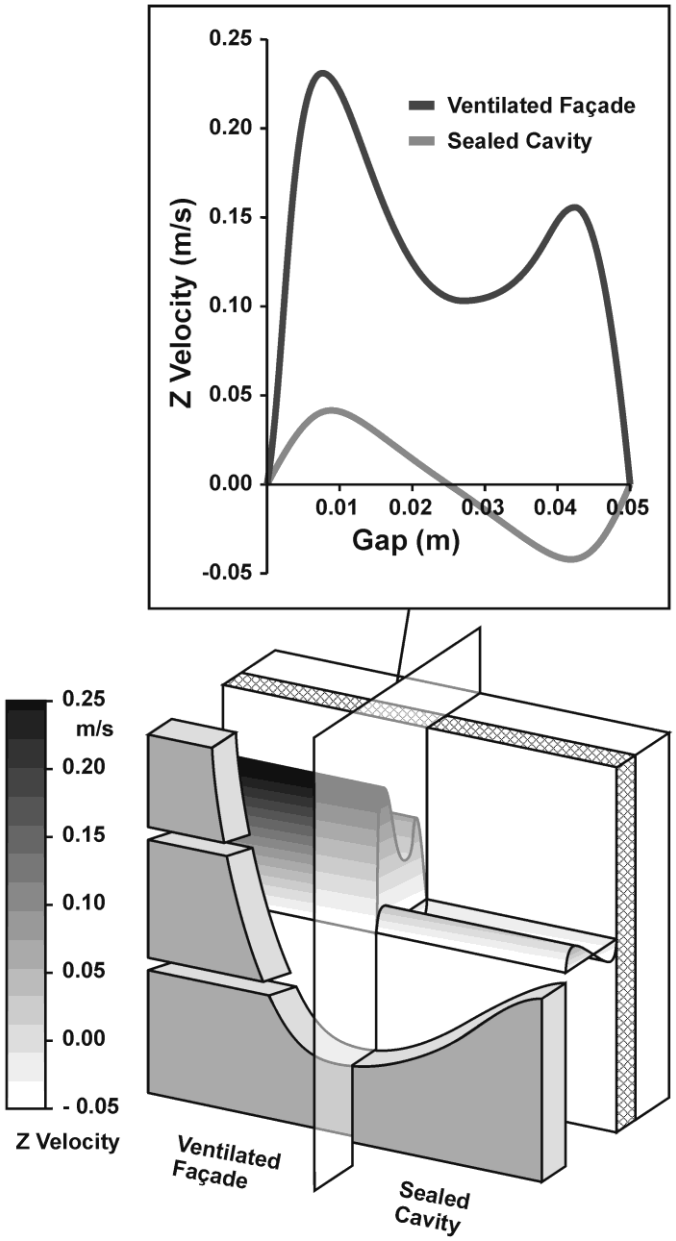

Fig. 8. Z velocity profiles at mid-height. OJVF vs. sealed cavity façade. Summer conditions (24ºC room, 30ºC exterior, 400 W/m^2 absorbed solar radiation)

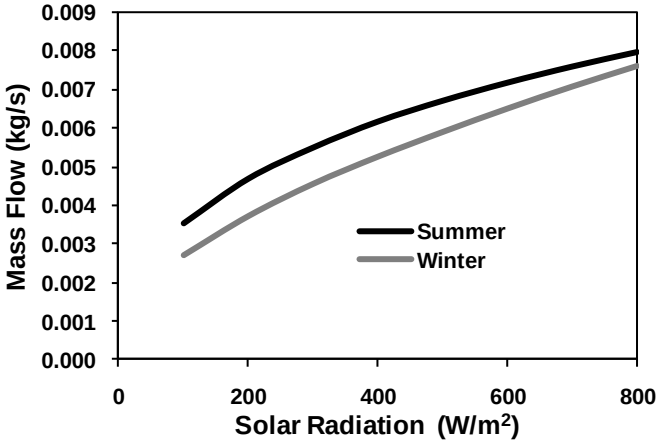

Fig. 9. Ventilation mass flow rate in function of absorbed solar radiation, at the central height of the OJVF. Calculated for a frontal section of one slab. Summer conditions (24ºC room, 30ºC exterior), winter conditions (24ºC room, 8ºC exterior)

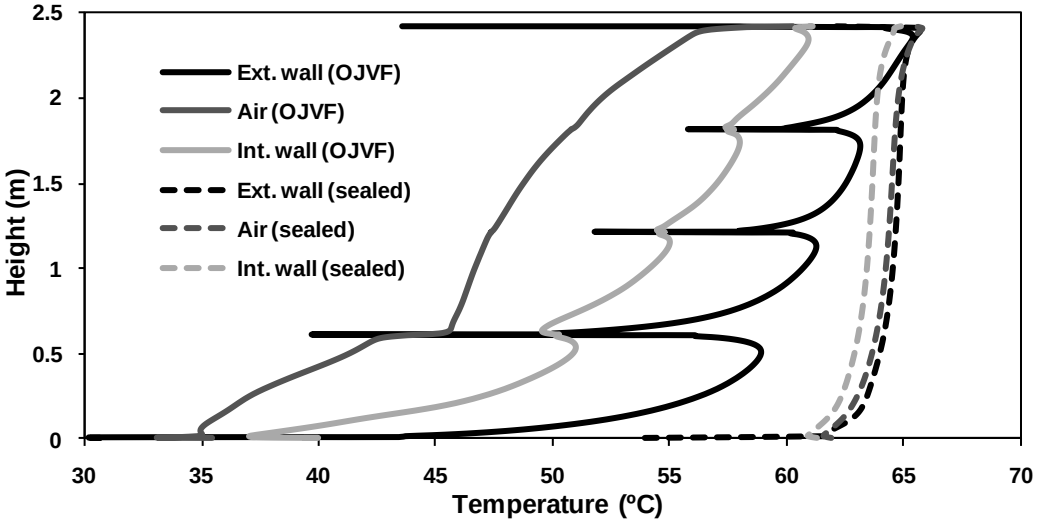

Fig. 10. Cavity temperature: OJVF vs. sealed façade. Summer conditions (24ºC room, 30ºC exterior, 400 W/m^2 absorbed solar radiation)

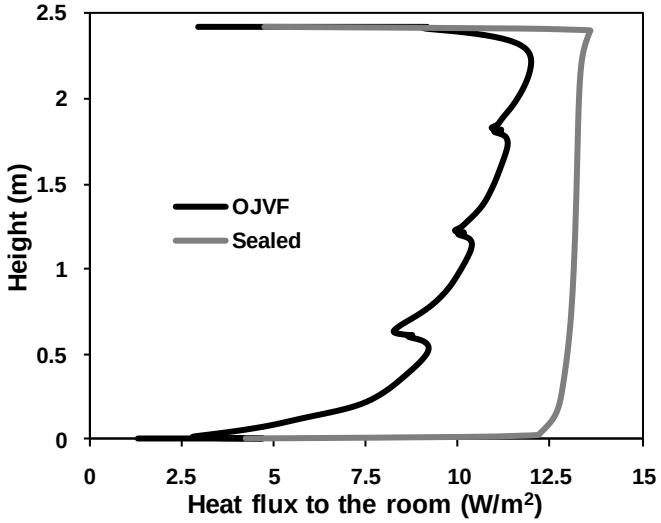

Fig. 11. Heat Flux to the room: OJVF vs. sealed façade. Summer conditions (24ºC room, 30ºC exterior, 400 W/m^2 absorbed solar radiation)

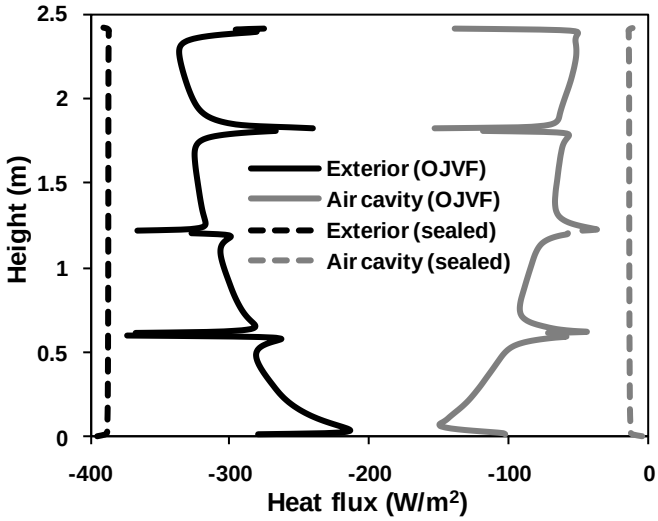

Fig. 12. Heat Fluxes on the external layer: OJVF vs. sealed façade. Summer conditions (24ºC room, 30ºC exterior, 400 W/m^2 absorbed solar radiation)

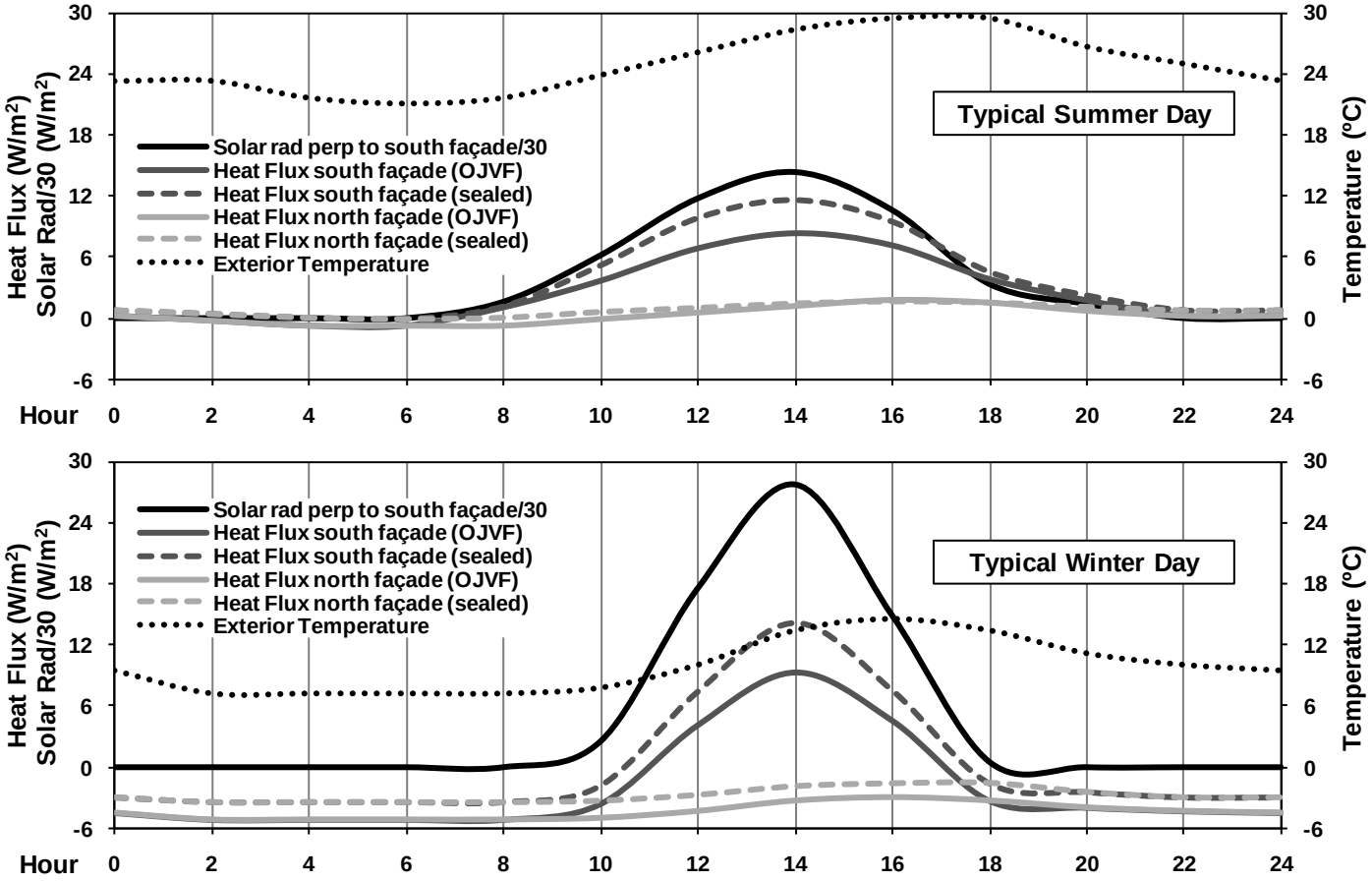

Fig. 13. Energy performance: OJVF vs. sealed façade. Typical summer and winter days.

Table 1
Thickness and thermal properties of the façade layers (from inside to outside)

Composition	Thickness [mm]	Density [kg/m^3]	Specific heat [J kg/K]	Conductivity [W/m K]	Emissivity
Gypsum	10	1800	831	0.81	
Brick wall	110	1800	840	0.52	
Insulation	30	40	1674	0.029	0.85
Air gap	50				
Slabs	10	2800	1000	3.5	0.9

Table 2
Heat transferred to the room in the typical days [Wh/m^2]

	South façade		North façade	
Summer	OJVF	Sealed	OJVF	Sealed
Day	455	613	66	101
Night	-16	18	-16	18
Energy req.	168	210	38	39
Winter	OJVF	Sealed	OJVF	Sealed
Day	108	255	-191	-114
Night	-471	-313	-471	-313
Energy req.	507	398	662	426

Figures and Table captions

Fig. 1. Open-joint ventilated façade (the joints are exaggerated in the drawing)

Fig. 2. Typical cross section of a sealed cavity and an open-joint ventilated façade (OJVF)

Fig. 3. Heat fluxes in a façade with an air cavity.

Fig. 4. Differences in heat transfer processes between a conventional sealed cavity façade and an OJVF.

Fig 5. Model domain. Dimensions and boundary conditions.

Fig. 6. Mesh over the slabs and horizontal and vertical joints.

Fig. 7. Horizontally averaged velocity magnitude and Z velocity component, at the middle vertical plane in the OJVF. Summer conditions (24ºC room, 30ºC exterior, 400 W/m^2 absorbed solar radiation)

Fig. 8. Z velocity profiles at mid-height. OJVF vs. sealed cavity façade. Summer conditions (24ºC room, 30ºC exterior, 400 W/m^2 absorbed solar radiation)

Fig. 9. Ventilation mass flow rate in function of absorbed solar radiation, at the central height of the OJVF. Calculated for a frontal section of one slab. Summer conditions (24ºC room, 30ºC exterior), winter conditions (24ºC room, 8ºC exterior)

Fig. 10. Cavity temperature: OJVF vs. sealed façade. Summer conditions (24ºC room, 30ºC exterior, 400 W/m^2 absorbed solar radiation)

Fig. 11. Heat Flux to the room: OJVF vs. sealed façade. Summer conditions (24ºC room, 30ºC exterior, 400 W/m^2 absorbed solar radiation)

Fig. 12. Heat Fluxes on the external layer: OJVF vs. sealed façade. Summer conditions (24ºC room, 30ºC exterior, 400 W/m^2 absorbed solar radiation)

Fig. 13. Energy performance: OJVF vs. sealed façade. Typical summer and winter days.

Table 1
Thickness and thermal properties of the façade layers (from inside to outside)

Table 2
Heat transferred to the room in the typical days [Wh/m^2]